Decentralized Spatial Partitioning Algorithms for Multi-Vehicle Systems Based on the Minimum Control Effort Metric

E. Bakolas[a,*]

[a] *Department of Aerospace Engineering and Engineering Mechanics, The University of Texas at Austin, Austin, Texas 78712-1221, USA*

Abstract

We consider the problem of characterizing a spatial partition of the position space of a team of vehicles with linear time-varying kinematics. The generalized metric that determines the proximity relations between the vehicles and an arbitrary target point in the partition space is the minimum control effort required for each vehicle to reach the latter point with zero miss distance and exactly zero velocity at a prescribed final time. We show that the solution to the generalized Voronoi partitioning problem can be associated with a special class of spatial partitions known as affine diagrams. Because the combinatorial complexity of the affine diagrams is comparable to the one of the standard Voronoi diagrams, their computation does not pose a significant challenge in applications of multi-vehicle systems. Subsequently, we propose an algorithm for the computation of the spatial partition, which is decentralized in the sense that each vehicle can compute an approximation of its own cell independently from the other vehicles from the same team without utilizing a common spatial mesh. Numerical simulations that illustrate the theoretical developments are also presented.

Keywords: Voronoi diagrams, spatial partitioning, multi-vehicle systems, minimum control effort

1. Introduction

This paper deals with a spatial partitioning problem for a team of vehicles with linear time-varying kinematics. The motivation for this type of problems stems from applications involving multi-vehicle systems, where the load of performing a particular set of tasks needs to be divided fairly among the different vehicles based on, for example, their locations and their steering capabilities (*spatial load balancing* [1, 2]). In this framework, a vehicle is associated with a subset of its operating environment, which we refer to as the *Region-of-Influence* (ROI), which consists of all the possible locations where a task can be carried out by this particular vehicle with less incurred cost than any other vehicle from the same team. The incurred cost will be measured in terms of the value function of a relevant optimal control problem [3, 4]. In contrast to our previous work on similar partitioning problems, which is based on centralized computational techniques, in this work, we propose a decentralized partitioning algorithm that allows each vehicle to independently compute its own ROI.

By using proximity metrics that correspond to the value functions of relevant optimal control problems, one can obtain spatial partitions that encode proximity information that succinctly captures the dynamic characteristics of the vehicles; something that can not be achieved with the use of other standard metrics found in the literature [5], which stem solely from geometric considerations. Some special classes of problems whose proximity metric corresponds to the value function of a relevant optimal control problem can be found in [6, 3, 7, 4, 8, 9]. With the exception of [9], in the majority of the available results, the motion of the vehicles is described by first order kinematic models. Ref. [9], on the other hand, deals with a class of generalized Voronoi partitioning problems for multi-vehicle systems with linear second order dynamics, where the proximity metric is the minimum control effort required for each vehicle to reach a neighborhood of a target point with a small terminal speed (soft terminal constraints). In this reference, it is shown that the solution to the partitioning problem can be directly associated with a particular class of power or affine diagrams, for the computation of which exact, yet centralized, algorithms exist in the literature. Consequently, by utilizing the techniques presented in [9], every vehicle will be unable to compute its ROI without, at the same time, computing by itself the ROIs of the other vehicles from the same team or receiving this information, via, say, an "all-to-all" type communication network.

In this work, we present a *decentralized* partitioning algorithm that computes an approximation of a spatial partition for a team of vehicles with second order linear time-varying kinematics and non-zero, in general, initial velocities based on the minimum control effort metric. Here the qualifier "decentralized" has the following meaning: with the utilization of the proposed algorithm, every vehicle will be able to compute its corresponding cell, or ROI, from the partition without computing at the same time the cells that correspond to other vehicles from the same team by utilizing a common spatial mesh. In this way, frugal use of the available resources is achieved. Moreover, in the definition of the proximity metric, we now explic-

*Corresponding author
Email address: bakolas@austin.utexas.edu (E. Bakolas)

itly require that each vehicle reaches an arbitrary target point with zero miss distance and with exactly zero terminal velocity at a given finite terminal time (hard terminal constraints), in contrast with [9].

In order to address the partitioning problem, we exploit the intrinsic connection of its solution, which is a subdivision of a flat two-dimensional manifold whose ambient space is a four-dimensional Euclidean space, with a special class of partitions known as affine diagrams[1], which subdivide the two-dimensional Euclidean plane. The desired spatial partition and the corresponding affine diagram contain the same amount of information about the proximity relations between the vehicles and arbitrary target points in the plane. It turns out that, under some mild assumptions, the affine diagram that is associated with the desired spatial partition is comprised of cells that are star-convex with respect to their corresponding generators[2]. The previous fact will allow us to utilize some recent results on the parallel computation of generalized Voronoi diagrams in normed spaces by Reem [11, 12] in order to develop a decentralized partitioning algorithm for the computation of this affine diagram.

The rest of the paper is organized as follows. Section 2 presents the formulation of the optimal control problem for a single vehicle. The partitioning problem for the multi-vehicle scenario is formulated and subsequently solved by means of a decentralized algorithm in Section 3. Section 4 presents numerical simulations, and finally, Section 5 concludes the paper with a summary of remarks.

2. Formulation of the Optimal Steering Problem

2.1. Notation

We first introduce some useful notation used throughout the paper. In particular, we denote by $\mathbb{R}^2$ and $\mathbb{R}^4$ the set of two- and four-dimensional vectors, respectively. In addition, we write $\mathbb{Z}_{>0}$ to denote the set of positive integers. We denote by $|\alpha|$ the Euclidean norm (the length) of a vector α and by $\langle\beta,\gamma\rangle$ the standard inner product of two vectors β and γ, where $\alpha,\beta,\gamma\in\mathbb{R}^\ell$, $\ell\in\{2,4\}$. The unit circle, that is, the set $\{\mathsf{e}\in\mathbb{R}^2:\ |\mathsf{e}|=1\}$, is denoted by $\mathbb{S}^1$. The space of square integrable functions $g(\cdot):[0,\tau]\mapsto\mathbb{R}^2$, for a given $\tau>0$, is denoted by $\mathcal{L}^2([0,\tau],\mathbb{R}^2)$. Furthermore, $\mathcal{L}^\infty([0,\tau],\mathbb{R}^{2\times 2})$ denotes the space of (almost everywhere) bounded functions $\mathbf{M}(\cdot):[0,\tau]\mapsto\mathbb{R}^{2\times 2}$. In addition, $\mathrm{bd}(\mathcal{A})$ and $\mathrm{int}(\mathcal{A})$ denote, respectively, the boundary and the interior of the set $\mathcal{A}$. We denote the fact that a symmetric matrix $\mathbf{A}$ is positive definite by writing $\mathbf{A}=\mathbf{A}^{\mathrm{T}}\succ\mathbf{0}$. Finally, given two points α and $\beta\in\mathbb{R}^2$, we denote by $[\alpha,\beta]$ the line segment from α to β and by $\Gamma(\alpha;\mathsf{e})$ the ray emanating from α that is parallel to $\mathsf{e}\in\mathbb{S}^1$.

[1] Affine diagrams are Voronoi-like partitions whose bisectors, that is, the curves that consist of the equidistant points from any two generators of the partition, are hyperplanes (or straight lines in the two-dimensional case) [10].

[2] A set is star-convex with respect to one of its points, if the line segment connecting this point with any other point in the set lies entirely in the same set.

2.2. Problem Formulation

We are given a team of n vehicles which are initially located at n distinct points, $\bar{\mathsf{x}}_i\in\mathbb{R}^2$, with prescribed initial velocities, $\bar{\mathsf{v}}_i\in\mathbb{R}^2$, where $i\in\mathcal{I}_n:=\{1,\ldots,n\}$. We denote by $\overline{\mathcal{X}}:=\{\bar{\mathsf{x}}_i\in\mathbb{R}^2,\ i\in\mathcal{I}_n\}$ and $\overline{\mathcal{V}}:=\{\bar{\mathsf{v}}_i\in\mathbb{R}^2,\ i\in\mathcal{I}_n\}$, respectively, the sets of the initial positions and velocities of all the vehicles. To simplify the presentation, we will assume that all the vehicles have the same dynamic characteristics (homogeneous team of vehicles). In particular, the motion of the i-th vehicle from the team, where $i\in\mathcal{I}_n$, is described by the following set of equations

$$\begin{aligned}\dot{\mathsf{x}}_i&=\mathsf{v}_i, & \mathsf{x}_i(0)&=\bar{\mathsf{x}}_i,\\ \dot{\mathsf{v}}_i&=-\mathbf{K}(t)\mathsf{x}_i-\mathbf{C}(t)\mathsf{v}_i+\mathbf{H}(t)u_i(t), & \mathsf{v}_i(0)&=\bar{\mathsf{v}}_i,\end{aligned}\qquad(1)$$

where $\mathsf{x}_i:=[x_i,\ y_i]^{\mathrm{T}}\in\mathbb{R}^2$ and $\mathsf{v}_i:=[v_i,\ w_i]^{\mathrm{T}}\in\mathbb{R}^2$ are, respectively, the position and velocity vectors of the i-th vehicle at time t. In addition, $u_i(\cdot)\in\mathcal{L}^2([0,\tau],\mathbb{R}^2)$ is the control input of the i-th vehicle. Furthermore, $\mathbf{K}(\cdot)$, $\mathbf{C}(\cdot)$, $\mathbf{H}(\cdot)\in\mathcal{L}^\infty([0,\tau],\mathbb{R}^{2\times 2})$. Moreover, we denote by $\mathsf{z}_i:=[\mathsf{x}_i^{\mathrm{T}},\ \mathsf{v}_i^{\mathrm{T}}]^{\mathrm{T}}$ and $\bar{\mathsf{z}}_i:=[\bar{\mathsf{x}}_i^{\mathrm{T}},\ \bar{\mathsf{v}}_i^{\mathrm{T}}]^{\mathrm{T}}$ the state of the i-th vehicle (concatenation of position and velocity vectors) at time t and $t=0$, respectively; the set of initial states of all the vehicles is denoted by $\overline{\mathcal{Z}}:=\{\bar{\mathsf{z}}_i\in\mathbb{R}^4:\ i\in\mathcal{I}_n\}$. The kinematics of the i-th vehicle can be written more compactly as follows:

$$\dot{\mathsf{z}}_i=\mathbf{A}(t)\mathsf{z}_i+\mathbf{B}(t)u_i(t),\quad \mathsf{z}_i(0)=\bar{\mathsf{z}}_i,\qquad(2)$$

where

$$\mathbf{A}(t):=\begin{bmatrix}\mathbf{0}_2 & \mathbf{I}_2\\ -\mathbf{K}(t) & -\mathbf{C}(t)\end{bmatrix},\qquad \mathbf{B}(t):=\begin{bmatrix}\mathbf{0}_2\\ \mathbf{H}(t)\end{bmatrix}.$$

Let us now define the *terminal position space* to be the flat two-dimensional manifold $\mathcal{X}_0:=\{[\mathsf{x}^{\mathrm{T}},\ \mathsf{v}^{\mathrm{T}}]^{\mathrm{T}}\in\mathbb{R}^4:\ \mathsf{v}=0\}$. Note that $\mathcal{X}_0$ is globally homeomorphic to $\mathbb{R}^2$. Next, we consider the problem of steering the i-th vehicle to a target point in $\mathcal{X}_0$.

Problem 1. *Given a fixed final time $\tau>0$ and a point $\mathsf{x}\in\mathbb{R}^2$, determine a control input $u_i^\circ(\cdot)\in\mathcal{L}^2(\mathbb{R}^2,[0,\tau])$ that minimizes the cost criterion*

$$J(u_i(\cdot)):=\tfrac{1}{2}\int_0^\tau|u_i(t)|^2\mathrm{d}t\qquad(3)$$

subject to the dynamic constraint (2) *and the following boundary conditions: $\mathsf{z}_i(0)=\bar{\mathsf{z}}_i$ and $\mathsf{z}_i(\tau)=\mathsf{z}(\mathsf{x})$, where $\mathsf{z}(\mathsf{x}):=[\mathsf{x}^T,\ 0]^T$, $\mathsf{z}(\mathsf{x})\in\mathcal{X}_0$.*

Remark 1 Note that in the definition of the cost criterion, we could have added a quadratic term penalizing the state of the i-th vehicle. However, it turns out that the quadratic optimization problem with the penalty on both the control and the state under the original dynamic constraints (2) can be transformed to a minimum control effort problem whose dynamic constraints are given by (2) after replacing the matrix $\mathbf{A}(t)$ with an appropriate matrix $\tilde{\mathbf{A}}(t)$ (for more details, the reader should refer to Theorem 2 [13, pp. 140–141]).

Assumption 1. *Let $\mathbf{\Phi}$ be the state transition matrix of the homogeneous system $\dot{\mathsf{z}}_i = \mathbf{A}(t)\mathsf{z}_i$, that is, the vector $\mathbf{\Phi}(t,0)\bar{\mathsf{z}}_i$ solves the initial value problem (2), when $u_i(\cdot) \equiv 0$. The controllability Grammian $\mathbf{W}(t)$ of the system described by Eq. (2), where*

$$\mathbf{W}(t) := \int_0^t \mathbf{\Phi}(0,\sigma)\mathbf{B}(\sigma)\mathbf{B}^T(\sigma)\mathbf{\Phi}^T(0,\sigma)\mathrm{d}\sigma, \qquad (4)$$

is positive definite at $t = \tau$, that is, $\mathbf{W}(\tau) = \mathbf{W}^T(\tau) \succ \mathbf{0}$.

Under Assumption 1, it can be shown that the optimal control $u_i^\circ(\cdot)$ that solves Problem 1 is a time-varying feedback law, which is given by (see, for example, Theorem 1 [13, p. 137])

$$u_i^\circ(t,\mathsf{x};\tau,\bar{\mathsf{z}}_i) = \mathbf{B}^{\mathrm{T}}(t)\mathbf{\Phi}^{\mathrm{T}}(0,t)\mathbf{W}^{-1}(\tau)(\mathbf{\Phi}(0,\tau)\mathsf{z}(\mathsf{x}) - \bar{\mathsf{z}}_i). \qquad (5)$$

Note that (5) can be written more compactly as follows

$$u_i^\circ(t,\mathsf{x};\tau,\bar{\mathsf{z}}_i) = \mathbf{M}(t;\tau)(\mathsf{z}(\mathsf{x}) - \zeta(\tau,\bar{\mathsf{z}}_i)), \qquad (6)$$

where

$$\begin{aligned}\mathbf{M}(t;\tau) &:= \mathbf{B}^{\mathrm{T}}(t)\mathbf{\Phi}^{\mathrm{T}}(0,t)\mathbf{W}^{-1}(\tau)\mathbf{\Phi}(0,\tau),\\ \zeta(\tau,\bar{\mathsf{z}}_i) &:= \mathbf{\Phi}(\tau,0)\bar{\mathsf{z}}_i,\end{aligned} \qquad (7)$$

Note that in the derivation of (6), we have used the fact that $\mathbf{\Phi}^{-1}(0,\tau) = \mathbf{\Phi}(\tau,0)$. We observe that the gains of the optimal control $u_i^\circ(\cdot)$ depend explicitly on the final time τ. Next, we define the value function of Problem 1, that is, the cost incurred during the transition of the i-th vehicle driven by the optimal control law $u_i^\circ(t,\mathsf{x};\tau,\bar{\mathsf{z}}_i)$, for $t \in [0,\tau]$, from $\bar{\mathsf{z}}_i \in \overline{\mathcal{Z}}$ to a state $\mathsf{z}(\mathsf{x}) \in \mathcal{X}_0$. We denote this function, which we refer to as the *minimum control effort metric*, by $J^\circ(\cdot) : \mathsf{x} \mapsto J^\circ(\mathsf{x};\tau,\bar{\mathsf{z}}_i)$, where

$$J^\circ(\mathsf{x};\tau,\bar{\mathsf{z}}_i) := \tfrac{1}{2}\int_0^\tau |u_i^\circ(t,\mathsf{x};\tau,\bar{\mathsf{z}}_i)|^2\mathrm{d}t. \qquad (8)$$

In light of Eq. (6), we get

$$J^\circ(\mathsf{x};\tau,\bar{\mathsf{z}}_i) := \langle(\mathsf{z}(\mathsf{x}) - \zeta(\tau,\bar{\mathsf{z}}_i)), \mathbf{P}(\tau)(\mathsf{z}(\mathsf{x}) - \zeta(\tau,\bar{\mathsf{z}}_i))\rangle, \qquad (9)$$

where

$$\mathbf{P}(\tau) := \tfrac{1}{2}\int_0^\tau \mathbf{M}^{\mathrm{T}}(t;\tau)\mathbf{M}(t;\tau)\mathrm{d}t. \qquad (10)$$

It is easy to show that

$$\mathbf{P}(\tau) = \tfrac{1}{2}\mathbf{\Phi}^{\mathrm{T}}(0,\tau)\mathbf{W}^{-1}(\tau)\mathbf{\Phi}(0,\tau), \qquad (11)$$

from which we can immediately conclude that $\mathbf{P}(\tau) = \mathbf{P}^{\mathrm{T}}(\tau) \succ \mathbf{0}$.

Remark 2 Note that both the expressions for the optimal control and the value function of the optimal steering problem given, respectively, in Eqs. (6) and (9) depend on the time duration, τ, of the desired state transition but not on the initial time, although the dynamics of the i-th vehicle depend, in general, on the time t explicitly. This is because, in the formulation of Problem 1, we have taken the initial time to be $t = 0$.

Proposition 1. *Suppose that Assumption 1 holds. Let $\tau > 0$ be given and let the matrix $\mathbf{P}(\tau) \in \mathbb{R}^{4\times4}$, which is defined in (10), be partitioned as follows*

$$\mathbf{P}(\tau) = \begin{bmatrix}\mathbf{P}_{11}(\tau) & \mathbf{P}_{12}(\tau)\\ \mathbf{P}_{12}^T(\tau) & \mathbf{P}_{22}(\tau)\end{bmatrix},$$

where $\mathbf{P}_{11}(\tau)$, $\mathbf{P}_{12}(\tau)$ and $\mathbf{P}_{22}(\tau) \in \mathbb{R}^{2\times2}$. Let also the vector $\zeta(\tau,\bar{\mathsf{z}}_i) \in \mathbb{R}^4$, which is defined in (7), be partitioned as follows

$$\zeta(\tau,\bar{\mathsf{z}}_i) = \left[\zeta_1^T(\tau,\bar{\mathsf{z}}_i), \quad \zeta_2^T(\tau,\bar{\mathsf{z}}_i)\right]^T,$$

where $\zeta_1(\tau,\bar{\mathsf{z}}_i)$ and $\zeta_2(\tau,\bar{\mathsf{z}}_i) \in \mathbb{R}^2$. Then, the value function of Problem 1 can be written as follows:

$$\begin{aligned}J^\circ(\mathsf{x};\tau,\bar{\mathsf{z}}_i) = {}& \langle(\mathsf{x} - \mathsf{q}(\tau,\bar{\mathsf{z}}_i), \mathbf{P}_{11}(\tau)(\mathsf{x} - \mathsf{q}(\tau,\bar{\mathsf{z}}_i))\rangle\\ &+ \delta(\tau,\bar{\mathsf{z}}_i),\end{aligned} \qquad (12)$$

where

$$\begin{aligned}\mathsf{q}(\tau,\bar{\mathsf{z}}_i) &:= \zeta_1(\tau,\bar{\mathsf{z}}_i) + \mathbf{P}_{11}^{-1}(\tau)\mathbf{P}_{12}(\tau)\zeta_2(\tau,\bar{\mathsf{z}}_i),\\ \delta(\tau,\bar{\mathsf{z}}_i) &:= \langle\zeta_2(\tau,\bar{\mathsf{z}}_i), \mathbf{Q}(\tau)\zeta_2(\tau,\bar{\mathsf{z}}_i)\rangle,\\ \mathbf{Q}(\tau) &:= \mathbf{P}_{22}(\tau) - \mathbf{P}_{12}^T(\tau)\mathbf{P}_{11}^{-1}(\tau)\mathbf{P}_{12}(\tau).\end{aligned} \qquad (13)$$

Proof. The fact that $\mathbf{P}(\tau) = \mathbf{P}^{\mathrm{T}}(\tau) \succ \mathbf{0}$ implies that $\mathbf{P}_{11}(\tau) = \mathbf{P}_{11}^{\mathrm{T}}(\tau) \succ \mathbf{0}$. Then, by completing the square, Eq. (9) yields

$$\begin{aligned}J^\circ(\mathsf{x};\tau,\bar{\mathsf{z}}_i) &= \langle\mathsf{x} - \zeta_1, \mathbf{P}_{11}(\mathsf{x} - \zeta_1)\rangle\\ &\quad - 2\langle\mathsf{x} - \zeta_1, \mathbf{P}_{12}\zeta_2\rangle\\ &\quad + \langle\zeta_2, \mathbf{P}_{22}\zeta_2\rangle\\ &= |\mathbf{P}_{11}^{1/2}(\mathsf{x} - \zeta_1)|^2\\ &\quad - 2\langle\mathbf{P}_{11}^{1/2}(\mathsf{x} - \zeta_1), \mathbf{P}_{11}^{-1/2}\mathbf{P}_{12}\zeta_2\rangle\\ &\quad + |\mathbf{P}_{11}^{-1/2}\mathbf{P}_{12}\zeta_2|^2\\ &\quad - |\mathbf{P}_{11}^{-1/2}\mathbf{P}_{12}\zeta_2|^2\\ &\quad + \langle\zeta_2, \mathbf{P}_{22}\zeta_2\rangle\\ &= |\mathbf{P}_{11}^{1/2}(\mathsf{x} - \zeta_1) - \mathbf{P}_{11}^{-1/2}\mathbf{P}_{12}\zeta_2|^2\\ &\quad + \langle\zeta_2, (\mathbf{P}_{22} - \mathbf{P}_{12}^{\mathrm{T}}\mathbf{P}_{11}^{-1}\mathbf{P}_{12})\zeta_2\rangle\\ &= |\mathbf{P}_{11}^{1/2}(\mathsf{x} - \zeta_1 - \mathbf{P}_{11}^{-1}\mathbf{P}_{12}\zeta_2)|^2\\ &\quad + \langle\zeta_2, (\mathbf{P}_{22} - \mathbf{P}_{12}^{\mathrm{T}}\mathbf{P}_{11}^{-1}\mathbf{P}_{12})\zeta_2\rangle,\end{aligned}$$

where we have dropped the arguments of ζ_k and $\mathbf{P}_{k\ell}$ to facilitate the presentation. The result follows readily. ■

Remark 3 Note that the function $J^\circ(\cdot) : \mathsf{x} \mapsto J^\circ(\mathsf{x};\tau,\bar{\mathsf{z}}_i)$ attains its minimum value at $\mathsf{x} = \mathsf{x}^\circ$, where $\mathsf{x}^\circ := \mathsf{q}(\tau,\bar{\mathsf{z}}_i)$. In particular,

$$J^\circ(\mathsf{x}^\circ;\tau,\bar{\mathsf{z}}_i) = \min_{\mathsf{x}\in\mathbb{R}^2} J^\circ(\mathsf{x};\tau,\bar{\mathsf{z}}_i) = \delta(\tau,\bar{\mathsf{z}}_i).$$

Note that the minimizer x° is, in general, different from the initial state of the i-th vehicle. This may appear counterintuitive at a first glance; one would expect the minimizer

of $J^\circ(\cdot)$ to be instead the initial position of the i-th vehicle, $\bar{\mathsf{x}}_i$. The important nuance here is that, according to the formulation of Problem 1, the terminal position has to be reached with zero terminal velocity. Consequently, a non-zero control effort is required, in general, even for the transition from $\bar{\mathsf{z}}_i$ to $\mathsf{z}(\bar{\mathsf{x}}_i)$, where $\mathsf{z}(\bar{\mathsf{x}}_i) = [\bar{\mathsf{x}}_i^{\mathrm{T}},\ 0]^{\mathrm{T}}$. These observations will play an important role in the subsequent analysis.

3. The Partitioning Problem

Next, we formulate the generalized Voronoi partitioning problem with respect to the minimum control effort metric.

Problem 2. *Let $\overline{\mathcal{Z}} := \{\bar{\mathsf{z}}_i \in \mathbb{R}^4,\ i \in \mathcal{I}_n\}$ be given. Then, determine a partition $\mathfrak{V} = \{\mathfrak{V}_i,\ i \in \mathcal{I}_n\}$ of $\mathcal{X}_0$ such that*

1. $\mathcal{X}_0 = \bigcup_{i\in\mathcal{I}_n} \mathfrak{V}_i$,
2. $\mathrm{int}(\mathfrak{V}_i) \cap \mathrm{int}(\mathfrak{V}_j) = \varnothing$, *for all* $i, j \in \mathcal{I}_n$, $i \neq j$,
3. *A point* $\mathsf{z}(\mathsf{x}) \in \mathcal{X}_0$, *where* $\mathsf{z}(\mathsf{x}) = [\mathsf{x}^T,\ 0]^T$, *belongs to* $\mathfrak{V}_i$ *if, and only if,* $J^\circ(\mathsf{x};\tau,\bar{\mathsf{z}}_i) \leq J^\circ(\mathsf{x};\tau,\bar{\mathsf{z}}_j)$, *for all* $j \in \mathcal{I}_n\backslash\{i\}$, *where* $J^\circ(\mathsf{x};\tau,\bar{\mathsf{z}}_\ell)$, $\ell \in \{i,j\}$, *is given by Eq.* (12).

Remark 4 Note that the proximity metric in Problem 2 is not a metric in the strict mathematical sense; for example, $J^\circ(\bar{\mathsf{x}}_i;\tau,\mathsf{z}(\bar{\mathsf{x}}_i)) \neq 0$, where $\mathsf{z}(\bar{\mathsf{x}}_i) = [\bar{\mathsf{x}}_i^{\mathrm{T}},\ 0]^{\mathrm{T}}$, in general.

3.1. Analysis of the Partitioning Problem

Let $\bar{\mathsf{z}}_i, \bar{\mathsf{z}}_j \in \overline{\mathcal{Z}}$ and let $\mathcal{B}_{ij}$ denote their common bisector in $\mathfrak{V}$, which is defined as the collection of all points $\mathsf{z}(\mathsf{x}) \in \mathcal{X}_0$ that are equidistant from $\bar{\mathsf{z}}_i$ and $\bar{\mathsf{z}}_j$ in terms of the minimum control effort metric $J^\circ(\cdot)$, that is, $J^\circ(\mathsf{x};\tau,\bar{\mathsf{z}}_i) = J^\circ(\mathsf{x};\tau,\bar{\mathsf{z}}_j)$. Equivalently, $\mathsf{z}(\mathsf{x}) \in \mathcal{B}_{ij}$ if, and only if,

$$\begin{aligned}\langle \mathsf{x} - \mathsf{q}(\tau,\bar{\mathsf{z}}_i), \mathbf{P}_{11}(\tau)(\mathsf{x} - \mathsf{q}(\tau,\bar{\mathsf{z}}_i))\rangle + \delta(\tau,\bar{\mathsf{z}}_i) = \\ \langle \mathsf{x} - \mathsf{q}(\tau,\bar{\mathsf{z}}_j), \mathbf{P}_{11}(\tau)(\mathsf{x} - \mathsf{q}(\tau,\bar{\mathsf{z}}_j))\rangle + \delta(\tau,\bar{\mathsf{z}}_j),\end{aligned}$$

which implies that

$$\begin{aligned}\langle \mathsf{q}(\tau,\bar{\mathsf{z}}_i), \mathbf{P}_{11}(\tau)\mathsf{q}(\tau,\bar{\mathsf{z}}_i)\rangle - 2\langle \mathsf{x}, \mathbf{P}_{11}(\tau)\mathsf{q}(\tau,\bar{\mathsf{z}}_i)\rangle + \delta(\tau,\bar{\mathsf{z}}_i) = \\ \langle \mathsf{q}(\tau,\bar{\mathsf{z}}_j), \mathbf{P}_{11}(\tau)\mathsf{q}(\tau,\bar{\mathsf{z}}_j)\rangle - 2\langle \mathsf{x}, \mathbf{P}_{11}(\tau)\mathsf{q}(\tau,\bar{\mathsf{z}}_j)\rangle + \delta(\tau,\bar{\mathsf{z}}_j).\end{aligned}$$

It follows that $\mathcal{B}_{ij}$ is determined by the following equation

$$\langle \mathsf{x}, \chi(\bar{\mathsf{z}}_i,\bar{\mathsf{z}}_j;\tau)\rangle = m(\bar{\mathsf{z}}_i,\bar{\mathsf{z}}_j;\tau), \tag{14}$$

where

$$\begin{aligned}\chi(\bar{\mathsf{z}}_i,\bar{\mathsf{z}}_j;\tau) &:= 2\mathbf{P}_{11}(\tau)(\mathsf{q}(\tau,\bar{\mathsf{z}}_j) - \mathsf{q}(\tau,\bar{\mathsf{z}}_i)),\\ m(\bar{\mathsf{z}}_i,\bar{\mathsf{z}}_j;\tau) &:= |\mathbf{P}_{11}^{1/2}(\tau)\mathsf{q}(\tau,\bar{\mathsf{z}}_j)|^2 - |\mathbf{P}_{11}^{1/2}(\tau)\mathsf{q}(\tau,\bar{\mathsf{z}}_i)|^2\\ &\quad + \delta(\tau,\bar{\mathsf{z}}_j) - \delta(\tau,\bar{\mathsf{z}}_i).\end{aligned}$$

Note that Eq. (14) states that the inner product of an arbitrary two-dimensional vector x with the constant vector $\chi(\bar{\mathsf{z}}_i,\bar{\mathsf{z}}_j;\tau)$ is always equal to the constant scalar $m(\bar{\mathsf{z}}_i,\bar{\mathsf{z}}_j;\tau)$. Therefore, unless $\chi(\bar{\mathsf{z}}_i,\bar{\mathsf{z}}_j;\tau) = 0$, that is, $\mathsf{q}(\tau,\bar{\mathsf{z}}_j) = \mathsf{q}(\tau,\bar{\mathsf{z}}_i)$, Eq. (14) describes a straight line in $\mathbb{R}^2$ that is perpendicular to the vector $\chi(\bar{\mathsf{z}}_i,\bar{\mathsf{z}}_j;\tau)$ and its distance from the origin is equal to $|m|/|\chi|$. Note that Eq. (14) can be written alternatively as follows

$$\langle \mathsf{z}(\mathsf{x}), \xi(\chi(\bar{\mathsf{z}}_i,\bar{\mathsf{z}}_j;\tau))\rangle = m(\bar{\mathsf{z}}_i,\bar{\mathsf{z}}_j;\tau), \tag{15}$$

where $\mathsf{z}(\mathsf{x}) := [\mathsf{x}^{\mathrm{T}},\ 0]^{\mathrm{T}}$ and $\xi(\chi) := [\chi^{\mathrm{T}},\ 0]^{\mathrm{T}}$. Note that Eq. (15) implies that $\mathsf{z}(\mathsf{x})$ belongs to the hyperplane in $\mathbb{R}^4$ that is perpendicular to the constant vector $\xi(\chi)$ and its distance from the origin is equal to $|m|/|\xi(\chi)| = |m|/|\chi|$.

Proposition 2. *Let $\tau > 0$ be given and let $\mathfrak{V} := \{\mathfrak{V}_i,\ i \in \mathcal{I}_n\}$ denote the generalized Voronoi diagram that solves Problem 2 for a given set of generators $\overline{\mathcal{Z}} := \{\bar{\mathsf{z}}_i,\ i \in \mathcal{I}_n\}$. Let us also consider a partition $\mathfrak{Q} := \{\mathfrak{Q}_i,\ i \in \mathcal{I}_n\}$ of $\mathbb{R}^2$ that is generated by the point-set $\overline{\mathcal{Q}} := \{\bar{\mathsf{q}}_i,\ i \in \mathcal{I}_n\}$ with respect to the proximity metric $J^\circ(\cdot) : \mathsf{x} \mapsto J^\circ(\mathsf{x};\tau,\bar{\mathsf{q}}_i,\delta_i)$, where*

$$J^\circ(\mathsf{x};\tau,\bar{\mathsf{q}}_i,\delta_i) := \langle \mathsf{x} - \bar{\mathsf{q}}_i, \mathbf{P}_{11}(\tau)(\mathsf{x} - \bar{\mathsf{q}}_i)\rangle + \delta_i, \tag{16}$$

$\bar{\mathsf{q}}_i := \mathsf{q}(\tau,\bar{\mathsf{z}}_i)$, $\delta_i := \delta(\tau,\bar{\mathsf{z}}_i)$ and where $\mathsf{q}(\cdot)$, $\delta(\cdot)$ are defined in Eq. (13) *and $\mathbf{P}_{11}(\tau) \in \mathbb{R}^{2\times 2}$ is a positive definite matrix, $\mathbf{P}_{11}(\tau) = \mathbf{P}_{11}^T(\tau) \succ \mathbf{0}$, which is defined in Proposition 1. Suppose that $\overline{\mathcal{Q}}$ consists of n distinct points in $\mathbb{R}^2$. Then, a point $\mathsf{z}(\mathsf{x}) \in \mathcal{X}_0$, where $\mathsf{z}(\mathsf{x}) = [\mathsf{x}^T,\ 0]^T$, belongs to the cell $\mathfrak{V}_i$ if, and only if, $\mathsf{x} \in \mathfrak{Q}_i$. In addition, $\mathfrak{Q} := \{\mathfrak{Q}_i,\ i \in \mathcal{I}_n\}$ is an affine diagram with combinatorial complexity $\Theta(n)$*[3].

Proof. Equations (12) and (16) imply that $J^\circ(\mathsf{x};\tau,\bar{\mathsf{z}}_i) = J^\circ(\mathsf{x};\tau,\bar{\mathsf{q}}_i,\delta_i)$, provided that $\bar{\mathsf{q}}_i = \mathsf{q}(\tau,\bar{\mathsf{z}}_i)$ and $\delta_i = \delta(\tau,\bar{\mathsf{z}}_i)$. Therefore, a point $\mathsf{z}(\mathsf{x}) \in \mathcal{X}_0$, where $\mathsf{z}(\mathsf{x}) = [\mathsf{x}^{\mathrm{T}},\ 0]^{\mathrm{T}}$, belongs to the cell $\mathfrak{V}_i$, where $\mathfrak{V}_i \in \mathfrak{V}$, if, and only if, $J^\circ(\mathsf{x};\tau,\bar{\mathsf{z}}_i) \leq J^\circ(\mathsf{x};\tau,\bar{\mathsf{z}}_j)$, for all $i \neq j$, or equivalently, $J^\circ(\mathsf{x};\tau,\bar{\mathsf{q}}_i,\delta_i) \leq J^\circ(\mathsf{x};\tau,\bar{\mathsf{q}}_j,\delta_j)$. Thus, $\mathsf{z}(\mathsf{x}) \in \mathfrak{V}_i$ if, and only if, $\mathsf{x} \in \mathfrak{Q}_i$, where $\mathfrak{Q}_i \in \mathfrak{Q}$.

Finally, let $\bar{\mathsf{q}}_i,\ \bar{\mathsf{q}}_j \in \overline{\mathcal{Q}}$, where $i \neq j$. Then, the bisector $\mathcal{B}_{ij}$ of $\bar{\mathsf{q}}_i$ and $\bar{\mathsf{q}}_j$ is determined by Eq. (14), which is the equation of a straight line in $\mathbb{R}^2$ given that, by hypothesis, $\bar{\mathsf{q}}_i \neq \bar{\mathsf{q}}_j$. Consequently, $\mathfrak{Q}$ is an affine diagram in $\mathbb{R}^2$. The result on the combinatorial complexity of $\mathfrak{Q}$ follows immediately from Theorem 18.2.3 in [10, p. 439]. ■

Remark 5 Proposition 2 states that the partitions $\mathfrak{V}$ and $\mathfrak{Q}$ are equivalent in terms of characterizing the proximity relations between the vehicles and arbitrary points in $\mathcal{X}_0$. For example, if a point $\mathsf{z}(\mathsf{x}) \in \mathcal{X}_0$, where $\mathsf{z}(\mathsf{x}) = [\mathsf{x}^{\mathrm{T}},\ 0]^{\mathrm{T}}$, belongs to $\mathfrak{V}_i$, then the point $\mathsf{x} \in \mathbb{R}^2$ will belong to $\mathfrak{Q}_i$, and vice versa. In addition, Proposition 2 essentially refines Proposition 4 from [9], where it is not explicitly required that neither the miss target distance nor the terminal speed be exactly zero. Using similar arguments to the ones in [9], one concludes that $\mathfrak{Q}$ can be computed in $\Theta(n\log n + n)$ time. The derivation of the previous bound is based, however, on the analysis of general classes of affine diagrams computed by means of centralized algorithms (the reader is referred to [10] for more details).

[3] We denote by $\Theta(f(n))$ the set of functions $F : \mathbb{Z}_{>0} \mapsto [0,\infty)$ for which there exist c_1, $c_2 > 0$ and $n_0 \in \mathbb{Z}_{>0}$ such that $c_1 f(n) \leq F(n) \leq c_2 f(n)$, for all $n \geq n_0$.

3.2. A Decentralized Spatial Partitioning Algorithm

Next, we present a decentralized algorithm, which instead of directly computing the partition $\mathfrak{V} = \{\mathfrak{V}_i,\ i \in \mathcal{I}_n\}$ generated by $\overline{\mathcal{Z}} \subset \mathbb{R}^4$, computes its "equivalent" partition $\mathfrak{Q}$ generated by $\overline{\mathcal{Q}} \subset \mathbb{R}^2$. We will henceforth assume, based on practical considerations, that our partition space is a compact and convex set $\mathcal{S} \subset \mathbb{R}^2$. Before we proceed, we make the following assumption:

Assumption 2. *Let $\mathcal{S}$ be a compact and convex set in $\mathbb{R}^2$ and let $\tau > 0$ and $\overline{\mathcal{Z}} = \{\bar{\mathsf{z}}_i \in \mathbb{R}^4,\ i \in \mathcal{I}_n\}$ be given. Let also $\bar{\mathsf{q}}_i := \mathsf{q}(\tau, \bar{\mathsf{z}}_i)$ and $\delta_i := \delta(\tau, \bar{\mathsf{z}}_i)$, for $i \in \mathcal{I}_n$, where $\mathsf{q}(\cdot)$ and $\delta(\cdot)$ are defined in Eq.* (13)*. Then $\bar{\mathsf{q}}_i$ is an interior point of $\mathcal{S}$, that is, $\bar{\mathsf{q}}_i \in \mathrm{int}(\mathcal{S})$, and*

$$\langle \bar{\mathsf{q}}_i - \bar{\mathsf{q}}_j, \mathbf{P}_{11}(\tau)(\bar{\mathsf{q}}_i - \bar{\mathsf{q}}_j)\rangle + \delta_j > \delta_i, \tag{17}$$

for all $i \in \mathcal{I}_n$ and $j \in \mathcal{I}_n\backslash\{i\}$, where $\mathbf{P}_{11}(\tau) \in \mathbb{R}^{2\times 2}$ is a positive definite matrix, $\mathbf{P}_{11}(\tau) = \mathbf{P}_{11}^T(\tau) \succ \mathbf{0}$, which is defined in Proposition 1.

Remark 6 Note that Assumption 2 requires that the vehicles are placed such that numerical singularities (when, for example, the cell of one or more generators in $\overline{\mathcal{Q}}$ has an empty interior) are avoided during the computation of the partition; in the computational geometry parlance, we assume that the generators are placed in (a form of) *general position*. It is easy to see that condition (17) is satisfied, for example, when the initial speeds of the vehicles are small compared to their initial relative distances.

Proposition 3. *Suppose that Assumption 2 holds and let $\mathfrak{Q}$ be the affine diagram generated by $\overline{\mathcal{Q}} = \{\bar{\mathsf{q}}_i,\ i \in \mathcal{I}_n\}$ with respect to the proximity metric $J^\circ(\cdot) : \mathsf{x} \mapsto J^\circ(\mathsf{x}; \tau, \bar{\mathsf{q}}_i, \delta_i)$, which is defined in Eq.* (16)*. Then, the point $\bar{\mathsf{q}}_i \in \overline{\mathcal{Q}}$ belongs to the interior of its corresponding cell $\mathfrak{Q}_i \in \mathfrak{Q}$, $\bar{\mathsf{q}}_i \in \mathrm{int}(\mathfrak{Q}_i)$. In addition, the set $\mathfrak{Q}_i$ is star-convex with respect to the point $\bar{\mathsf{q}}_i$, that is, for every point $\mathsf{x} \in \mathfrak{Q}_i$, the line segment $[\bar{\mathsf{q}}_i, \mathsf{x}]$ lies entirely in $\mathfrak{Q}_i$, for all $i \in \mathcal{I}_n$.*

Proof. In light of Eq. (17), it follows that $J^\circ(\bar{\mathsf{q}}_i; \tau, \bar{\mathsf{q}}_i, \delta_i) < J^\circ(\bar{\mathsf{q}}_i; \tau, \bar{\mathsf{q}}_j, \delta_j)$, for all $j \in \mathcal{I}_n\backslash\{i\}$, which implies that $\bar{\mathsf{q}}_i$ is an interior point of $\mathfrak{Q}_i$, $\bar{\mathsf{q}}_i \in \mathrm{int}(\mathfrak{Q}_i)$. Each cell of the affine diagram $\mathfrak{Q}$ corresponds to the finite intersection of closed half-planes in $\mathbb{R}^2$. Consequently, the cell $\mathfrak{Q}_i$ is a convex set, which along with the fact that $\bar{\mathsf{q}}_i \in \mathrm{int}(\mathfrak{Q}_i)$ imply that $\mathfrak{Q}_i$ is actually a star-convex set with respect to the point $\bar{\mathsf{q}}_i$, for all $i \in \mathcal{I}_n$. ■

Remark 7 Proposition 3 states that, under Assumption 2, the point $\bar{\mathsf{q}}_i$ belongs to the interior of the cell $\mathfrak{Q}_i$. This result is quite intuitive given that the point $\bar{\mathsf{q}}_i$ is the minimizer of $J^\circ(\cdot; \tau, \bar{\mathsf{q}}_i, \delta_i)$, as we have already highlighted in Remark 3. Consequently, one would expect $\bar{\mathsf{q}}_i$ to be an interior point of the cell $\mathfrak{Q}_i$ given that, by definition, the interior of this set consists of points that are "closer," in terms of the minimum control effort metric, to $\bar{\mathsf{q}}_i$ than any other generator from the set $\overline{\mathcal{Q}}$. Later on, we will exploit this fact to develop a decentralized algorithm that solves Problem 2.

In light of Proposition 3, for each point $\mathsf{x} \in \mathfrak{Q}_i$, the line segment $[\bar{\mathsf{q}}_i, \mathsf{x}]$ will lie within the cell $\mathfrak{Q}_i$. Conversely, let us assume that there exists a point y that belongs to the ray $\Gamma(\bar{\mathsf{q}}_i; \mathsf{e})$ such that $J^\circ(\mathsf{y}; \tau, \bar{\mathsf{q}}_j, \delta_j) < J^\circ(\mathsf{y}; \tau, \bar{\mathsf{q}}_i, \delta_i)$, where $j \in \mathcal{I}_n\backslash\{i\}$. Then, no point of the ray $\Gamma(\mathsf{y}; \mathsf{e})$ that lies after the point y will belong the cell $\mathfrak{Q}_i$, that is, $\Gamma(\mathsf{y}; \mathsf{e}) \cap \mathfrak{Q}_i = \varnothing$. Next, we propose an algorithm that, for a given $\mathsf{e} \in \mathbb{S}^1$, seeks for the furthest point from $\bar{\mathsf{q}}_i$ along the ray $\Gamma(\bar{\mathsf{q}}_i; \mathsf{e})$, call it $\mathsf{x}_{\mathrm{bd}}(\mathsf{e}, \bar{\mathsf{q}}_i)$, such that

$$J^\circ(\mathsf{x}_{\mathrm{bd}}(\mathsf{e}, \bar{\mathsf{q}}_i); \tau, \bar{\mathsf{q}}_i, \delta_i) \leq J^\circ(\mathsf{x}_{\mathrm{bd}}(\mathsf{e}, \bar{\mathsf{q}}_i); \tau, \bar{\mathsf{q}}_j, \delta_j),$$

for all $j \in \mathcal{I}_n\backslash\{i\}$. Note that $\mathsf{x}_{\mathrm{bd}}(\mathsf{e}, \bar{\mathsf{q}}_i)$ corresponds to the intersection of the ray $\Gamma(\bar{\mathsf{q}}_i; \mathsf{e})$ with the boundary of the cell $\mathfrak{Q}_i$, $\mathrm{bd}(\mathfrak{Q}_i)$. Actually, it turns out that $\mathrm{bd}(\mathfrak{Q}_i) = \{\mathsf{x}_{\mathrm{bd}}(\mathsf{e}, \bar{\mathsf{q}}_i),\ \mathsf{e} \in \mathbb{S}^1\}$. To characterize a discrete approximation of $\mathrm{bd}(\mathfrak{Q}_i)$, we will borrow some ideas from [11, 12] for the computation of generalized Voronoi partitions in normed spaces. The approach presented in [11, 12] is based on a bisection algorithm that is applied along families of rays emanating from each generator. Because the proximity metric in these references is assumed to be a norm, it turns out that the cells of the partition are sets that are star convex with respect to their corresponding generators as a direct consequence of the triangle inequality. This is also true for the affine diagram $\mathfrak{Q}$ in our case, in light of Proposition 3, although the proximity metric $J^\circ(\cdot)$ in Problem 2 is not necessarily a metric in the strict mathematical sense, as is highlighted in Remark 4.

Next, we present the key steps of the proposed decentralized partitioning algorithm. In particular, we consider an $1 \times N$ mesh, which furnishes a finite approximation of the unit circle $\mathbb{S}^1$, call it $\mathcal{E}$. Then, we characterize the point $\mathsf{x}_{\mathrm{bd}}(\mathsf{e}, \bar{\mathsf{q}}_i) \in \mathrm{bd}(\mathfrak{Q}_i)$, for each unit vector $\mathsf{e} \in \mathcal{E}$. To this aim, we employ a bisection algorithm along the ray $\Gamma(\bar{\mathsf{q}}_i; \mathsf{e})$, for each $\mathsf{e} \in \mathcal{E}$, as suggested in [11, 12]. Next, we summarize the main steps of the utilized algorithm:

Step 1: Initially, we take $\mathsf{x}_{\mathrm{bd}}(\mathsf{e}, \bar{\mathsf{q}}_i)$ to be the point $\mathsf{x}^{[0]}(\mathsf{e})$ that corresponds to the intersection of $\Gamma(\bar{\mathsf{q}}_i; \mathsf{e})$ with the boundary $\mathrm{bd}(\mathcal{S})$ of the partition space $\mathcal{S}$. We set $\mathcal{J}^{[0]}(\mathsf{e}) := J^\circ(\mathsf{x}^{[0]}(\mathsf{e}); \tau, \bar{\mathsf{q}}_i, \delta_i)$ and $\rho^{[0]}(\mathsf{e}) := |\bar{\mathsf{q}}_i - \mathsf{x}^{[0]}(\mathsf{e})|$.

Step 2: If $\mathcal{J}^{[0]}(\mathsf{e}) \leq J^\circ(\mathsf{x}^{[0]}(\mathsf{e}); \tau, \bar{\mathsf{q}}_j, \delta_j)$, for all $j \in \mathcal{I}_n\backslash\{i\}$, then $\mathsf{x}_{\mathrm{bd}}(\mathsf{e}, \bar{\mathsf{q}}_i) = \mathsf{x}^{[0]}(\mathsf{e})$. Otherwise, we set $\rho^{[1]}(\mathsf{e}) := \frac{1}{2}\rho^{[0]}(\mathsf{e})$ to obtain a new point $\mathsf{x}^{[1]}(\mathsf{e}) := \bar{\mathsf{q}}_i + \rho^{[1]}(\mathsf{e})\mathsf{e}$. Then, we set $\mathcal{J}^{[1]}(\mathsf{e}) := J^\circ(\mathsf{x}^{[1]}(\mathsf{e}); \tau, \bar{\mathsf{q}}_i, \delta_i)$ and $\Delta\rho(\mathsf{e}) := \big|\rho^{[0]}(\mathsf{e}) - \rho^{[1]}(\mathsf{e})\big|$.

Step 3: If $\mathcal{J}^{[1]}(\mathsf{e}) \leq J^\circ(\mathsf{x}^{[0]}(\mathsf{e}); \tau, \bar{\mathsf{q}}_j, \delta_j)$, for all $j \in \mathcal{I}_n\backslash\{i\}$, then we set $\rho^{[2]}(\mathsf{e}) := \rho^{[1]}(\mathsf{e}) + \frac{1}{2}\Delta\rho(\mathsf{e})$, and $\rho^{[2]}(\mathsf{e}) := \rho^{[1]}(\mathsf{e}) - \frac{1}{2}\Delta\rho(\mathsf{e})$ otherwise. In this way, we obtain a new point $\mathsf{x}^{[2]}(\mathsf{e}) := \bar{\mathsf{q}}_i + \rho^{[2]}(\mathsf{e})\mathsf{e}$, which is closer to the desired point, $\mathsf{x}_{\mathrm{bd}}(\mathsf{e}, \bar{\mathsf{q}}_i)$. Subsequently, we set $\mathcal{J}^{[2]}(\mathsf{e}) := J^\circ(\mathsf{x}^{[2]}(\mathsf{e}); \tau, \bar{\mathsf{q}}_i, \delta_i)$, and $\Delta\rho(\mathsf{e}) := \big|\rho^{[1]}(\mathsf{e}) - \rho^{[2]}(\mathsf{e})\big|$.

Step 4: We repeat the previous steps until

$$|\mathsf{x}_{\mathrm{bd}}(\mathsf{e}, \bar{\mathsf{q}}_i) - \mathsf{x}^{[\bar{k}]}(\mathsf{e})| < \varepsilon \ \text{ or } \ k > \bar{k}, \tag{18}$$

for some given threshold $\varepsilon > 0$ and a positive integer $\bar{k}$, to obtain a finite sequence of points, $\{\mathsf{x}^{[k]}(\mathsf{e}) :\ k \in \mathcal{I}_{\bar{k}}\}$, where $\mathcal{I}_{\bar{k}} := \{1, \ldots, \bar{k}\}$. It is easy to show that when $k = \bar{k}$, we

have

$$|\mathsf{x}_{\mathrm{bd}}(\mathsf{e},\bar{\mathsf{q}}_i)-\mathsf{x}^{[\bar{k}]}(\mathsf{e})|\leq|\mathsf{x}^{[0]}(\mathsf{e})-\bar{\mathsf{q}}_i|/2^{\bar{k}}.$$

Therefore, the first condition in (18) is satisfied, if we take

$$\bar{k}>(\ln|\mathsf{x}^{[0]}(\mathsf{e})-\bar{\mathsf{q}}_i|-\ln\varepsilon)/\ln 2. \tag{19}$$

Step 5: We repeat Steps 1-4, for all $\mathsf{e}\in\mathcal{E}$, in order to obtain a point-set $\mathrm{bd}_{\mathcal{E}}(\mathfrak{Q}_i):=\{\mathsf{x}_{\mathrm{bd}}(\mathsf{e},\bar{\mathsf{q}}_i),\ \mathsf{e}\in\mathcal{E}\}$ that constitutes a discrete approximation of the boundary $\mathrm{bd}(\mathfrak{Q}_i)$ of the cell $\mathfrak{Q}_i$. The pseudo-code of the previously described computational scheme is given in Algorithm 1.

As shown in [11, 12], the proposed decentralized partitioning algorithm has, in general, time complexity $\mathcal{O}(n^2)$, where n is the number of vehicles, although in practice it can actually run in time $\mathcal{O}(n)$. It should be highlighted at this point that the accuracy of the obtained approximation of the partition $\mathfrak{Q}$ via the proposed decentralized algorithm, and thus the corresponding running time, depends on a number of other parameters besides the number of vehicles, including the fineness of the mesh $\mathcal{E}$ and the convergence threshold ε.

It should also be mentioned that in this work, we do not necessarily assume the existence of a communication network that would allow the vehicles to exchange information about their positions and velocities in the presence of certain communication constraints. We assume instead that the vehicles can sense the positions and measure the velocities of the other vehicles. Consequently, our algorithm, which is decentralized as we have already explained, is not distributed.

Algorithm 1 A decentralized algorithm that computes an approximation of the boundary of the cell $\mathfrak{Q}_i\in\mathfrak{Q}$

Input: A point-set $\overline{\mathcal{Q}}\subset\mathrm{int}(\mathcal{S})$
Output: A discrete approximation of $\mathrm{bd}(\mathfrak{Q}_i)$
%% Initialization:
for all $\mathsf{e}\in\mathcal{E}$ **do**
  $\mathsf{x}^{[0]}(\mathsf{e})\leftarrow\Gamma(\bar{\mathsf{q}}_i;\mathsf{e})\cap\mathrm{bd}(\mathcal{S})$
  $\rho^{[0]}(\mathsf{e})\leftarrow|\mathsf{x}^{[0]}(\mathsf{e})-\bar{\mathsf{q}}_i|$
  $\mathcal{J}^{[0]}(\mathsf{e})\leftarrow J^{\circ}(\mathsf{x}^{[0]}(\mathsf{e});\tau,\bar{\mathsf{q}}_i,\delta_i)$
  if $\mathcal{J}^{[0]}(\mathsf{e})\leq J^{\circ}(\mathsf{x}^{[0]}(\mathsf{e});\tau,\bar{\mathsf{q}}_j,\delta_j),\ \forall j\in\mathcal{I}_n\backslash\{i\}$ **then**
    $\mathcal{E}\leftarrow\mathcal{E}\backslash\{\mathsf{e}\}$
    $\mathsf{x}_{\mathrm{bd}}(\mathsf{e},\bar{\mathsf{q}}_i)\leftarrow\mathsf{x}^{[0]}(\mathsf{e})$
  else
    $\rho^{[1]}(\mathsf{e})\leftarrow\frac{1}{2}\rho^{[0]}(\mathsf{e}),\ \ \Delta\rho(\mathsf{e})\leftarrow\left|\rho^{[0]}(\mathsf{e})-\rho^{[1]}(\mathsf{e})\right|$
  end if
end for
$k\leftarrow 0$
%% Begin Iterative Process:
for all $\mathsf{e}\in\mathcal{E}$ **do**
  while $k<\bar{k}$ **do**
    $k\leftarrow k+1$
    $\mathsf{x}^{[k]}(\mathsf{e})\leftarrow\bar{\mathsf{q}}_i+\rho^{[k]}(\mathsf{e})\mathsf{e}$
    $\mathcal{J}^{[k]}(\mathsf{e})\leftarrow J^{\circ}(\mathsf{x}^{[k]}(\mathsf{e});\tau,\bar{\mathsf{q}}_i,\delta_i)$
    if $\mathcal{J}^{[k]}(\mathsf{e})\leq J^{\circ}(\mathsf{x}^{[k]}(\mathsf{e});\tau,\bar{\mathsf{q}}_j,\delta_j),\ \forall j\in\mathcal{I}_n\backslash\{i\}$ **then**
      $\rho^{[k+1]}(\mathsf{e})\leftarrow\rho^{[k]}(\mathsf{e})+\frac{1}{2}\Delta\rho(\mathsf{e})$
    else
      $\rho^{[k+1]}(\mathsf{e})\leftarrow\rho^{[k]}(\mathsf{e})-\frac{1}{2}\Delta\rho(\mathsf{e})$
    end if
    $\Delta\rho(\mathsf{e})\leftarrow\left|\rho^{[k+1]}(\mathsf{e})-\rho^{[k]}(\mathsf{e})\right|$
  end while
  $\mathsf{x}_{\mathrm{bd}}(\mathsf{e},\bar{\mathsf{q}}_i)\leftarrow\mathsf{x}^{[k]}(\mathsf{e})$
end for

4. Numerical Simulations

In this section, we present simulation results that illustrate the previously presented theoretical developments. We consider a team of $n=10$ vehicles with double integrator kinematics. In particular,

$$\begin{aligned}\dot{\mathsf{x}}_i&=\mathsf{v}_i, &\mathsf{x}_i(0)&=\bar{\mathsf{x}}_i,\\ \dot{\mathsf{v}}_i&=u_i(t), &\mathsf{v}_i(0)&=\bar{\mathsf{v}}_i,\end{aligned} \tag{20}$$

where $i\in\mathcal{I}_{10}$. In this case, one can compute analytically the optimal control (see, for example, [14, pp. 558-561]), which is given by

$$\begin{aligned}u_i^{\circ}(t,\mathsf{x};\tau,\bar{\mathsf{z}}_i)&=a(\mathsf{x};\tau,\bar{\mathsf{z}}_i)+tb(\mathsf{x};\tau,\bar{\mathsf{z}}_i),\\ a(\mathsf{x};\tau,\bar{\mathsf{z}}_i)&:=\tfrac{6}{\tau^2}(\mathsf{x}-\bar{\mathsf{x}}_i-\tau\bar{\mathsf{v}}_i)+\tfrac{2}{\tau}\bar{\mathsf{v}}_i,\\ b(\mathsf{x};\tau,\bar{\mathsf{z}}_i)&:=-\tfrac{12}{\tau^3}(\mathsf{x}-\bar{\mathsf{x}}_i-\tau\bar{\mathsf{v}}_i)-\tfrac{6}{\tau^2}\bar{\mathsf{v}}_i.\end{aligned} \tag{21}$$

Moreover, it follows, after substituting (21) in (8), that

$$\begin{aligned}J^{\circ}(\mathsf{x};\tau,\bar{\mathsf{z}}_i)&:=\tfrac{6}{\tau^3}|\mathsf{x}-\mathsf{q}(\tau,\bar{\mathsf{z}}_i)|^2+\delta(\tau,\bar{\mathsf{v}}_i),\\ \mathsf{q}(\tau,\bar{\mathsf{z}}_i)&:=\bar{\mathsf{x}}_i+\tfrac{\tau}{2}\bar{\mathsf{v}}_i,\quad \delta(\tau,\bar{\mathsf{v}}_i):=\tfrac{1}{2\tau}|\bar{\mathsf{v}}_i|^2.\end{aligned} \tag{22}$$

Figure 1 illustrates the solution to Problem 2 for $\tau=2$. The red crosses and the black arrows in Figure 1 denote, respectively, the initial positions $\bar{\mathsf{x}}_i\in\overline{\mathcal{X}}$ and velocities $\bar{\mathsf{v}}_i\in\overline{\mathcal{V}}$ of the vehicles. Furthermore, the magenta crosses correspond to the point-set $\overline{\mathfrak{Q}}$. For the computation of the partition illustrated in Figure 1, we have employed a naive centralized approximation algorithm. The latter algorithm amounts to the following steps: First, we discretize the partition space into a uniform fine mesh $\mathcal{G}$, which consists of 400×400 nodes. Subsequently, we assign to each node, $n_{\mathcal{G}}$, of the mesh $\mathcal{G}$ the index i of the vehicle for which $J^{\circ}(\mathsf{x}(n_{\mathcal{G}});\tau,\bar{\mathsf{z}}_i)\leq J^{\circ}(\mathsf{x}(n_{\mathcal{G}});\tau,\bar{\mathsf{z}}_j)$, for all $j\in\mathcal{I}_n\backslash\{i\}$, where $\mathsf{x}(n_{\mathcal{G}})$ denotes the location of the node $n_{\mathcal{G}}$ in the plane. This naive partitioning scheme has time complexity $\mathcal{O}(n|\mathcal{G}|)$, where $|\mathcal{G}|$ denotes the number of nodes of the spatial mesh [15]. Typically, the size of the mesh depends on the number of vehicles; the higher the number of vehicles, the finer the mesh should be. The green dashed lines in Fig. 1 correspond to the standard Voronoi diagram generated by the point-set $\overline{\mathcal{X}}$. Alternatively, one can utilize the so-called *direct diffusion* algorithm to compute an approximation of the desired spatial partition on the same mesh. The main idea behind the direct diffusion algorithm is to sweep the two-dimensional spatial mesh in four alternating orderings. During each sweep, the neighboring nodes of each node $n_{\mathcal{G}}$ are assigned to the "closest" generator. The process terminates when no changes on the assignment of any node $n_{\mathcal{G}}$ can occur (the algorithm has

converged). If an eight-connectivity scheme is employed for the characterization of the neighboring relations between the different nodes, then it can be easily shown that the diffusion algorithm has time complexity $\mathcal{O}(32|\mathcal{G}|)$, in contrast with the naive partitioning algorithm whose computation time is $\mathcal{O}(n|\mathcal{G}|)$ as we have already mentioned. Note that the advantages of the diffusion algorithm will become apparent only when the number of vehicles, n, is sufficiently large.

Next, we present the results of numerical simulations based on the decentralized partitioning algorithm presented in Section 3.2. In particular, Figure 2 illustrates a cell of the partition $\mathfrak{Q}$, which was computed independently by its corresponding vehicle. For the computation of this cell, we have used a discrete approximation of $\mathbb{S}^1$, $\mathcal{E}$, which is induced by a uniform discrete mesh on the interval $[0, 2\pi]$, $\mathcal{T}$. For our simulations, we have considered a coarse mesh of 50 nodes (Fig. 2(a)) and a less coarse mesh of 100 nodes (Fig. 2(b)) and we have taken $\varepsilon = 0.01$. The approximation of the cell obtained with the use of the less coarse mesh is actually very close to the one obtained via the naive centralized partitioning algorithm, which utilizes a fine spatial mesh (Fig. 1).

Figure 3 illustrates the results of a performance comparison between the decentralized, the naive and the direct diffusion partitioning algorithms. Note that the purpose of this comparison analysis is to highlight some important trends rather than being exhaustive. In particular, Figures 3(a)-3(c) illustrate the running time, denoted by t_{exec}, of the three algorithms versus the number of nodes, N, of the utilized spatial mesh $\mathcal{G}$ for three scenarios with $n = 10$, $n = 32$ and $n = 60$, respectively. In particular, N equals the number of nodes of the one-dimensional mesh, $\mathcal{T}$, that is utilized by the decentralized algorithm, whereas the naive and the direct diffusion partitioning algorithms utilize a two-dimensional spatial mesh with $|\mathcal{G}| = N^2$ nodes. Note that the decentralized algorithm computes only the cell illustrated in Fig. 2(b), whereas the naive and the direct diffusion algorithms compute the whole partition given that they cannot compute cells independently. The previous observation along with the fact that the size of $\mathcal{T}$ (one dimensional mesh) is much smaller than the size of $\mathcal{G}$ (two-dimensional spatial mesh) explain the significantly lower running time of the proposed decentralized algorithm.

5. Conclusion

In this paper, we have addressed a spatial partitioning problem that is relevant to applications of multi-vehicle systems. The proximity metric of the proposed spatial partition is the minimum control effort required to steer a vehicle with linear time-varying kinematics to a target point with exactly zero miss distance and zero terminal velocity (soft landing) at a given (finite) final time. We have shown that the solution to this partitioning problem can be associated with a class of affine diagrams of modest combinatorial complexity. For the computation of this affine diagram, we have utilized a decentralized partitioning algorithm that allows each vehicle to compute an approximation of its own cell independently from the other vehicles from the same team without utilizing a common spatial mesh. Future work includes the development of decentralized partitioning algorithms for problems involving multi-vehicle systems with nonlinear dynamics as well as distributed partitioning algorithms, where information about the positions and velocities of the vehicles is relayed among them by means of a communication network in the presence of certain communication constraints.

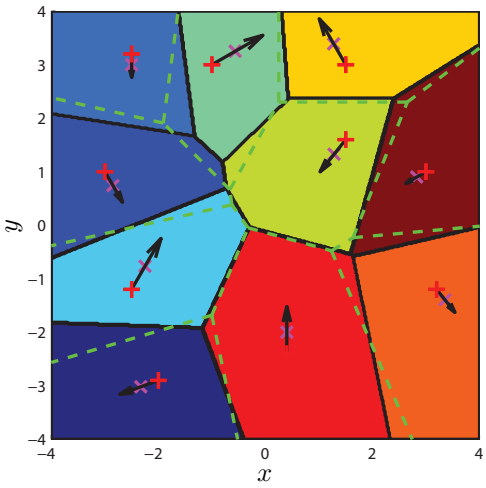

Figure 1: A spatial partition for a team of ten vehicles with respect to the minimum control effort metric computed via a naive centralized algorithm. The green dashed lines correspond to the standard Voronoi diagram generated by the point-set $\overline{\mathcal{X}}$.

Acknowledgements

The author would like to thank the anonymous reviewers for their constructive comments and suggestions. The author would also like to thank Jhanani Selvakumar for her help with the implementation of the direct diffusion algorithm.

References

[1] J. Cortes, Coverage optimization and spatial load balancing by robotic sensor networks, IEEE Transactions on Automatic Control 55 (3) (2010) 749–754.

[2] M. Pavone, A. Arsie, E. Frazzoli, F. Bullo, Distributed algorithms for environment partitioning in mobile robotic networks, IEEE Transactions on Automatic Control 56 (8) (2011) 1834–1848.

[3] E. Bakolas, P. Tsiotras, The Zermelo-Voronoi diagram: a dynamic partition problem, Automatica 46 (12) (2010) 2059–2067.

[4] E. Bakolas, P. Tsiotras, Optimal partitioning for spatiotemporal coverage in a drift field, Automatica 49 (7) (2013) 2064–2073.

[5] A. Okabe, B. Boots, K. Sugihara, S. N. Chiu, Spatial Tessellations: Concepts and Applications of Voronoi Diagrams, 2nd Edition, John Wiley and Sons Ltd, West Sussex, England, 2000.

[6] K. Sugihara, Voronoi diagrams in a river, International Journal of Computational Geometry and Applications 2 (1) (1992) 29–48.

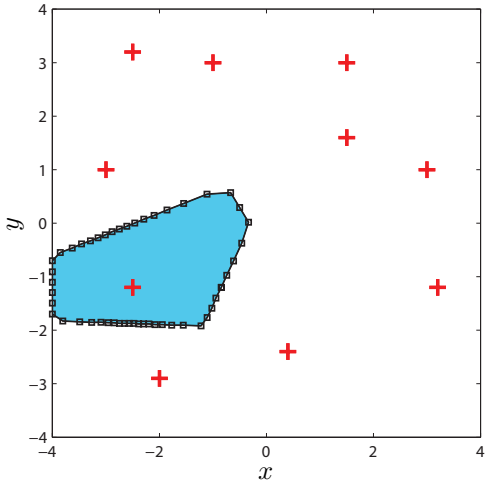

(a) Coarse approximation of a cell of $\mathfrak{Q}$.

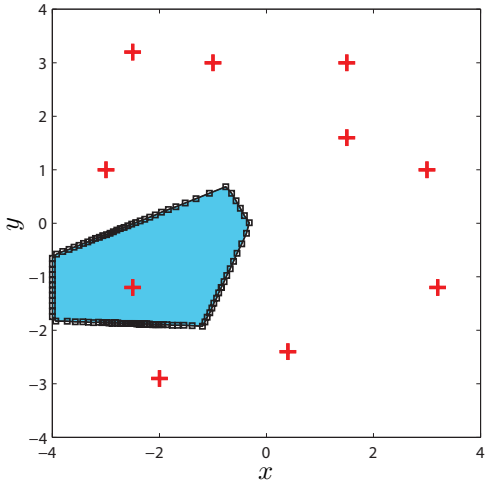

(b) Fine approximation of a cell of $\mathfrak{Q}$.

Figure 2: A particular cell from $\mathfrak{Q}$ computed via the decentralized partitioning algorithm using a coarse and a fine one-dimensional mesh, $\mathcal{T}$, consisting of 50 and 100 nodes, respectively.

[7] K. Sugihara, Why are Voronoi diagrams so fruitful in application?, in: ISVD 2011, 2011, p. 14.

[8] Y. Ru, S. Martinez, Coverage control in constant flow environments based on a mixed energy-time metric, Automatica 49 (9) (2013) 2632–2640.

[9] E. Bakolas, Optimal partitioning for multi-vehicle systems using quadratic performance criteria, Automatica 49 (11) (2013) 3377–3383.

[10] J.-D. Boissonnat, M. Yvinec, Algorithmic Geometry, Cambridge University Press, Cambridge, United Kingdom, 1998.

[11] D. Reem, An algorithm for computing Voronoi diagrams of general generators in general normed spaces, in: ISVD '09, 2009, pp. 144 –152.

[12] D. Reem, On the possibility of simple parallel computing of Voronoi diagrams and Delaunay graphs, arXiv:1212.1095.

[13] R. W. Brockett, Finite Dimensional Linear Systems, John Wiley & Sons, Inc., New York, USA, 1970.

[14] R. H. Battin, An Introduction to the Mathematics and Methods of Astrodynamics, AIAA, Reston, VA, 1999.

[15] T. Nishida, S. Ono, K. Sugihara, Direct diffusion method for the construction of generalized Voronoi diagrams, in: ISVD 2007, 2007, pp. 145–151.

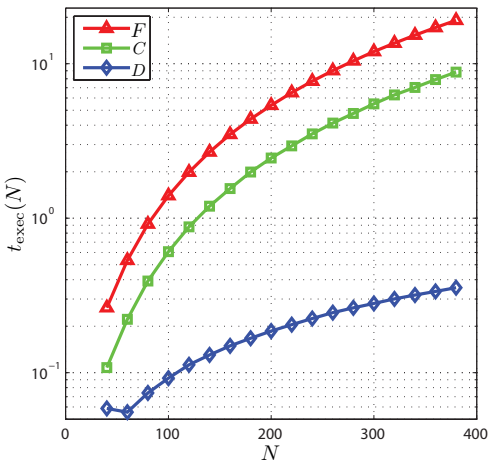

(a) The scenario with $n = 10$.

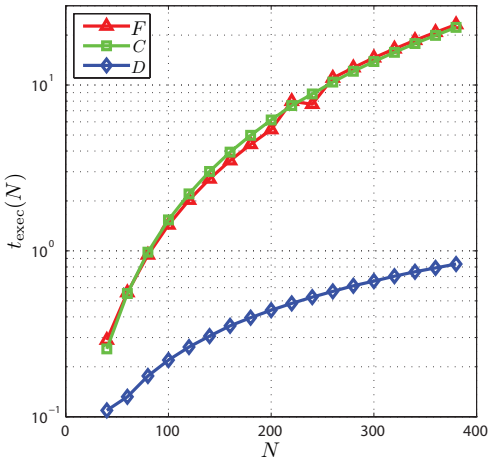

(b) The scenario with $n = 32$.

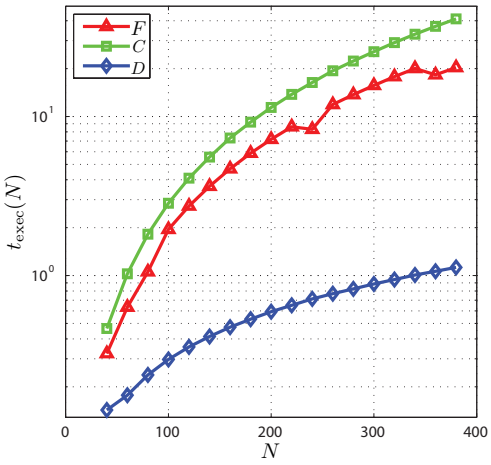

(c) The scenario with $n = 60$.

Figure 3: Running time of the three partitioning algorithms (the blue, the green, and the red curves correspond, respectively, to the decentralized, the naive, and the direct diffusion partitioning algorithms).